Research Paper

Luteolin attenuates the chemoresistance of osteosarcoma through inhibiting the PTN/β-catenin/MDR1 signaling axis by upregulating miR-384

Tao Qin [a,1], Wenjing Zhu [b,c,1], Xiaoli Kan [d], Ling Li [a], Dapeng Wu [a,*,2]

[a] Department of Oncology, Qingdao Municipal Hospital, Qingdao University, Qingdao, China
[b] Clinical Research Center, Qingdao Municipal Hospital, Qingdao University, Qingdao, China
[c] Department of Respiratory and Critical Care Medicine, Qingdao Municipal Hospital, Qingdao University, Qingdao, China
[d] Department of Gynecology, Qingdao Central Hospital, Qingdao University, Qingdao, China

ARTICLE INFO

ABSTRACT

Multidrug resistance (MDR) remains a critical bottleneck in successful treatment of osteosarcoma (OS). Luteolin is a flavonoid compound that has been verified to increase the sensitivity to antineoplastic drugs in many tumors. However, its roles in reversing MDR of OS and the potential underlying mechanisms remain largely unknown. In this study, we demonstrated that luteolin enhances cellular chemosensitivity to doxorubicin and cisplatin both in OS cells and xenograft models, and it could increase the miR-384 level and downregulate the PTN expression. Additionally, target analysis confirmed that miR-384 directly modulates PTN expression, and subsequent mechanistic analysis verified that miR-384 could inhibit the MDR of OS cells through suppressing the PTN/β-catenin/MDR1 signaling axis. Further analysis revealed treatment of sensitive MG63 cells with luteolin effectively packaged miR-384 into secreted exosomes and the exosomes could improve doxorubicin response in doxorubicin-resistant MG63/DOX cells. Our study confirmed that luteolin exerts MDR reversal effect against OS cells by regulating PTN expression via miR-384 and it may be a promising therapeutic agent for chemoresistant OS via its targeting of the PTN/β-catenin/MDR1 axis.

1. Introduction

Osteosarcoma (OS), characterized by strong invasiveness and rapid disease progression, is the most common primary bone malignancy [1]. Although the past decades have witnessed more therapeutic strategies including improved surgical techniques, multi-agent chemotherapy and target therapy, the OS prognosis remains unsatisfactory, especially in patients with metastatic or recurrent tumors. Among all the causes of failure in OS treatment, multi-drug resistance (MDR) is a key factor that limits the therapeutic efficacy. Thus, there is an urgent need to elucidate the mechanisms underlying OS chemoresistance and identify novel drugs to overcome MDR.

Since traditional Chinese herbal extract becomes one of the research hotspots nowadays, novel bioactive components with natural origins may be promising candidates for cancer therapy. Luteolin (3,4,5,7-tetrahydroxyflavone) is a dietary flavonoid compound extracted from several traditional Chinese medicines such as radix scutellariae, platycodon grandiflorum, dandelion, lonicera japonica, et al. Numerous studies have demonstrated that luteolin possesses many beneficial pharmacological properties including anticancer, antioxidant, antibacterial and anti-inflammatory effects, etc [2]. In traditional Chinese medicine, plants rich in luteolin have been used for the treatment of inflammatory diseases, hypertension, and tumors [3,4]. Luteolin has been reported to possess many antitumor properties including anti-proliferation, chemosensitizion, and radiosensitization in a variety of tumors, which has attracted increasing interest [5–9]. As for chemoresistance, luteolin has been suggested to potentiate the sensitivity of ovarian cancer, colorectal cancer, non-small cell lung cancer cells

---

and esophageal cancer to chemotherapeutic drugs [8,10–14]. In osteosarcoma, Wang et al. demonstrated luteolin could inhibit cell proliferation and induce apoptosis of osteosarcoma effectively in a dose-dependent manner [15]. Zhang et al. demonstrated that luteolin could induce autophagy and enhance doxorubicin-induced autophagy through upregulating beclin1 in OS cells [16]. Nevertheless, no evidence of luteolin on the chemoresistance of osteosarcoma has been reported.

Pleiotrophin (PTN) is a heparin-binding growth factor with various biological functions including cellular differentiation, proliferation, and metastasis. A meta-analysis concluded PTN expression has been demonstrated to be associated with poor survival outcomes in a variety of tumors [17]. In our previous study, we demonstrated PTN promoted chemoresistance in OS cells by upregulating P-glycoprotein (P-gp) through activating the ALK/GSK3β/β-catenin signaling pathway [18]. Additionally, our team further demonstrated the role of PTN in modulating resistance to doxorubicin in osteosarcoma [19]. As for the correlation between luteolin and PTN, evidence from a xenograft model and cell-based study verified that luteolin functions through regulating the miR-384/PTN axis in colorectal cancer [20]. Thus, we wondered whether luteolin could modulate the chemoresistance of osteosarcoma through miR-384 and PTN. MicroRNAs (miRNAs, miRs) are a class of endogenous short (∼22 nucleotides) noncoding RNA molecules that bind to the 3′-untranslated region (3′-UTR) of a target gene. miRNAs play critical roles in many biological events including cell differentiation, proliferation and apoptosis through post-transcriptionally regulating the expression of downstream target genes. Studies have suggested the involvement of miRNAs in the antineoplastic effects induced by luteolin [21–23]. In osteosarcoma, miR-384 overexpression was reported to inhibit invasion, migration, viability and promote apoptosis of osteosarcoma cells [24–26]. Nevertheless, the effect of miR-384 on the chemoresistance of osteosarcoma is still elusive. So we were wondering whether luteolin could influence the chemoresistance of OS through miR-384 and PTN. In the present study, we performed a series of functional assays to determine whether luteolin influences the chemoresistance of OS and explore the molecular mechanisms luteolin affects the cellular sensitivity.

2. Materials and methods

2.1. Cell culture and doxorubicin resistance induction

MG63 and U2OS cells were purchased from the Chinese Academy of Sciences Cell Bank (Shanghai, China). Normal human osteoblast hFOB1.19 cell line was purchased from Procell Life Science & Technology Co., Ltd (Wuhan, China). All tumor cells were cultured in Dulbecco's modified Eagle's medium (DMEM, Hyclone, South Logan, UT, USA) supplemented with 10% fetal bovine serum (FBS, Gibco, Rockford, MD, USA) and 1% penicillin–streptomycin at 37 °C in a 5% CO_2 incubator. The hFOB1.19 cells were grown in DMEM F12 nutrient mixture (DMEM/F12, Procell) supplemented with 0.3 mg/ml geneticin (G418), 10% FBS and 1% penicillin–streptomycin in a humidified incubator with 95% air and 5% CO2 at 34℃. Chemotherapeutic agents (doxorubicin and cisplatin) were obtained from Selleck Chemicals (Houston, TX, USA). Doxorubicin-resistant MG63/DOX cells were established as described previously [18]. Briefly, the parental MG63 cell line was cultured in the medium with increasing doses of doxorubicin from 5 nM to 100 nM step by step. Once cells could be freely dividing in the medium containing 100 nM doxorubicin, they were considered doxorubicin-resistant.

2.2. Quantitative real-time polymerase chain reaction (qRT-PCR)

Total RNA was extracted using a miRcute miRNA Isolation Kit and reversely transcribed to cDNA with a miRcute Plus miRNA First-Strand cDNA Synthesis Kit (Tiangen Biotech, Beijing, China) in accordance with the manufacturer's protocols. qRT-PCR was performed on a LightCycler480 Real-Time PCR System (Roche, Switzerland). The relative expression level of miR-384 was normalized to that of U6 small nuclear RNA, and the fold change was quantified using the $2^{-\Delta\Delta CT}$ method.

2.3. Cell viability assay

Cell viability was examined by Cell Counting Kit-8 (CCK-8, Dojindo Laboratories, Shanghai, China) assay. Cells with corresponding treatment were seeded into 96-well plates at a density of 4×10^3 cells/well and cultured with various drugs at 37 °C. At a specific time point, the cells were incubated with CCK-8 solution for 90 min. The absorbance at 450 nm was measured by a microplate reader (Bio-Rad, Hercules, CA, USA).

2.4. Luciferase reporter assay

Luciferase reporter gene plasmids containing the wild-type (WT) or mutant-type (MUT) 3′-untranslated region (3′-UTR) of PTN were constructed as follows. 3′-UTR segments of PTN that were predicted to interact with miR-384 were amplified by PCR and then inserted into the reporter vector pmir-GLO (Promega, Madison, WI, USA), and the resulted recombinant plasmid was named as pmir-PTN-WT. For the mutant (MUT) pmir-PTN construct, we replaced five nucleotides of the 3′-UTR within the seed sequence of miR-384-binding site and the resulted plasmid was named as pmir-PTN-Mut. Indicated cells were seeded into 24-well plates and transfected with reporter plasmids containing luciferase. Following transfection for 48 h, the cells were lysed and the Firefly and Renilla luciferase activities were measured using the Dual-Luciferase Reporter Assay System (Promega). The activity of Firefly luciferase was normalized by the Renilla luciferase activity.

2.5. Plasmid construction and cell transfection

To knockdown PTN in vitro, we chose the short hairpin RNA exhibiting the best PTN knockdown efficiency as previously verified [18]. The sequences of shRNA, miR-384 mimic, miR-384 inhibitor, and their control miRNAs were listed in Table 1. PTN cDNA was amplified by PCR and cloned into the pcDNA3.1 vector to generate PTN overexpression plasmids. To conduct cell transfection assays, cells were cultured in six-well plates and reached about 70%–80% confluence. Then the RNA oligonucleotides (mimic NC, miR-384 mimic, inhibitor NC, or miR-384 inhibitor), luciferase reporters (pmir-PTN-WT, pmir-PTN-Mut), or PTN overexpression plasmids were transiently transfected into the cells with Lipofectamine 2000 reagent (Invitrogen, Carlsbad, CA, USA) in accordance with the manufacturer's guidelines.

2.6. Cellular apoptosis assay

For apoptotic analysis, transfected cells were seeded into six-well plates and harvested after incubation with 0.2 μM doxorubicin or 2 μM cisplatin for 48 h. Cells were harvested by trypsinization and resuspended in binding buffer. Then cells were double-stained with Annexin V-FITC and propidium iodide (PI, Sanjian Biotech, Tianjin, China) and analyzed on a flow cytometer (Beckman, Brea, CA, USA).

Table 1
Information of the qPCR primer sequences and mimic/inhibitor sequences.

qPCR primer name	Sequence (5′-3′)
miR-384 (Forward)	TGTTAAATCAGGAATTTTAA
miR-384 (Reverse)	TGTTACAGGCATTATGAA
PTN (Forward)	GGGGAGAATGTGACCTGAAC
PTN (Reverse)	AGGGCTTGGA GATGGTGA
β-actin (Forward)	GTGGACATCCGCAAAGAC
β-actin (Reverse)	AAAGGGTGTAACGCAACTA
U6 (Forward)	CTCGCTTCGGCAGCACA
U6 (Reverse)	AACGCTTCACGAATTTGCGT
mimic/inhibitor name	**Sequence (5′-3′)**
PTN shRNA	TCAAGCAGAATCTAAGAAG
miR-384 mimic	AUUCCUAGAAAUUGUUCAUA
miR-384 inhibitor	UAUGAACAAUUUCUAGGAAU
miR-384 mimic NC	UUCUCCGAACGUGUCACGU
miR-384 inhibitor NC	CAGUACUUUUGUGUAGUACAA

2.7. Exosome isolation

Cells were cultured in exosome-free conditioned medium for 48 h and the cell supernatant was centrifuged at 4 °C, $500 \times g \times 10$ min, and $12,000 \times g \times 20$ min to remove cellular debris in turn. The supernatant was then gathered and centrifuged at ultra-high speed $(100,000 \times g) \times 2$ h using a 0.22-μm well filter (Millipore). Exosomes were collected with the pellet resuspended in PBS and stored at −80 °C.

2.8. Exosome identification

Purified exosomes were fixed with glutaraldehyde and then loaded onto carbon-coated copper grids. For electron microscopy analysis, copper grids with exosomes were stained by 2% phosphotungstic acid for 2 min. After air-drying, the samples were placed into the HT7700 transmission electron microscopy (TEM, Hitachi, Tokyo, Japan). Exosome images were captured with TEM, and the sizes were quantified by ZetaView (Particle Metrix, Meerbusch, Germany). The protein markers (CD63 and CD81) of exosomes were confirmed by Western blot analysis.

2.9. Xenograft experiment

Twenty-four female BALB/c nude mice of 6-weeks old were raised in pathogen-free conditions at 23 ± 1 °C and 58 ± 6% humidity. MG63/DOX cells in the logarithmic phase were harvested and suspended in 100 μL PBS at a concentration of 5×10^6 cells/ml. Cells were subcutaneously inoculated in the left hind flanks of nude mice. Mice were randomly divided into four groups (n = 6) and performed with different interventions. Tumor sizes were recorded every three days using a caliper until natural death or study termination (day 28) and calculated with the following formula: volume = $0.5 \times$ length $\times$ width^2. All procedures were conducted according to the protocols approved by the Animal Care and Use Committee of Qingdao Municipal Hospital.

2.10. Western blot analysis

Cells for protein extraction were lysed with RIPA buffer in the presence of protease inhibitors. The protein concentration was examined using the BCA protein assay kit (Beyotime Biotechnology, Beijing, China) and proteins were separated by SDS-PAGE. Then proteins were transferred to polyvinylidene difluoride (PVDF) membranes and blocked with Tris-buffered saline containing 5% non-fat milk. The blots were probed with primary antibodies against PTN (1:1000, Abcam, Cambridge, MA, USA), β-catenin (1:4000, Abcam), ALK (1:2000, Abcam), phospho-GSK3β at serine 9 (1:500, Abcam), P-glycoprotein (1:500, Proteintech, Chicago, IL,

USA), β-actin (1:2000, Abcam), α-tubulin(1:5000, Abcam) overnight at 4 °C. Then the blots were probed with the appropriate horse radish peroxidase (HRP)-conjugated secondary antibodies (1:5000, Santa Cruz Biotechnology, Dallas, TX, USA) for 90 min at room temperature and visualized using an enhanced chemiluminescence detection system.

2.11. Immunohistochemistry

Immunohistochemical assays were performed using paraffin-embedded sections as described previously [18].

2.12. Statistical analysis

Statistical analyses in this study were performed with SPSS 21.0 software (SPSS, Chicago, IL, USA), and data were presented as the mean ± standard deviation. Two-tailed Student's t-tests and one-way analysis of variance (ANOVA) were used for analyzing the statistical significance of differences between two or more groups. P value less than 0.05 was considered to be statistically significant.

3. Result

3.1. Effect of luteolin on OS cells in vitro

The morphology of doxorubicin-resistant MG63/DOX cells and the parental MG63 cells was shown in Fig. 1A. Cell proliferation assays were performed to examine cell growth curves and the half maximal inhibitory concentration (IC50) values of doxorubicin on MG63 and MG63/DOX cells were 0.58 μM and 4.21 μM, respectively (Fig. 1B). Cell viability assays showed the IC50 value of hFOB1.19 cells to luteolin was close to those in MG63 and U2OS cells (IC50 = 58.91 μM, 59.61 μM and 34.1 μM, respectively, Fig. 1C). We also demonstrated MG63/DOX cells possess higher resistance to luteolin than MG63 and U2OS cells (Fig. 1C). Moreover, chemosensitivity assays were performed to investigate whether luteolin influences drug resistance in OS cells. As shown in Fig. 1D and 1E, luteolin at concentrations of 1/2 IC50 values significantly decreased the chemoresistance to doxorubicin and cisplatin in the MG63, MG63/DOX and U2OS cells.

3.2. PTN is a direct target of miR-384

To investigate whether miR-384 played a role in modulating chemoresistance of OS cells, qRT-PCR was firstly used to detect miR-384 expression in OS cells. Our results showed that miR-384 was significantly downregulated in chemoresistant MG63/DOX cells compared with the parental sensitive MG63 cells, suggesting miR-384 may be involved in the chemoresistance of OS cells (Fig. 2A).

Given that miRNAs exert biological functions by regulating the expression of their target genes, we took advantage of the prediction algorithm TargetScan analysis (https://targetscan.org) to predict the potential targets of miR-384. PTN, a heparin-binding neurotrophic growth factor implicated in the tumorigenesis of numerous human malignancies, was identified as a direct target of miR-384. PTN contained potential miR-384 target sites in their 3′-UTRs and the seed sequences for miR-384 in the 3′-UTRs of PTN were shown in Fig. 2B.

Furthermore, we explored the effect of luteolin stimulation on miR-384 and PTN expression. We observed that the expression level of miR-384 could be enhanced in OS cells treated with the 50% IC50 concentration of luteolin in OS cells (Fig. 2C). Our results also showed luteolin treatment resulted in a significant decrease in
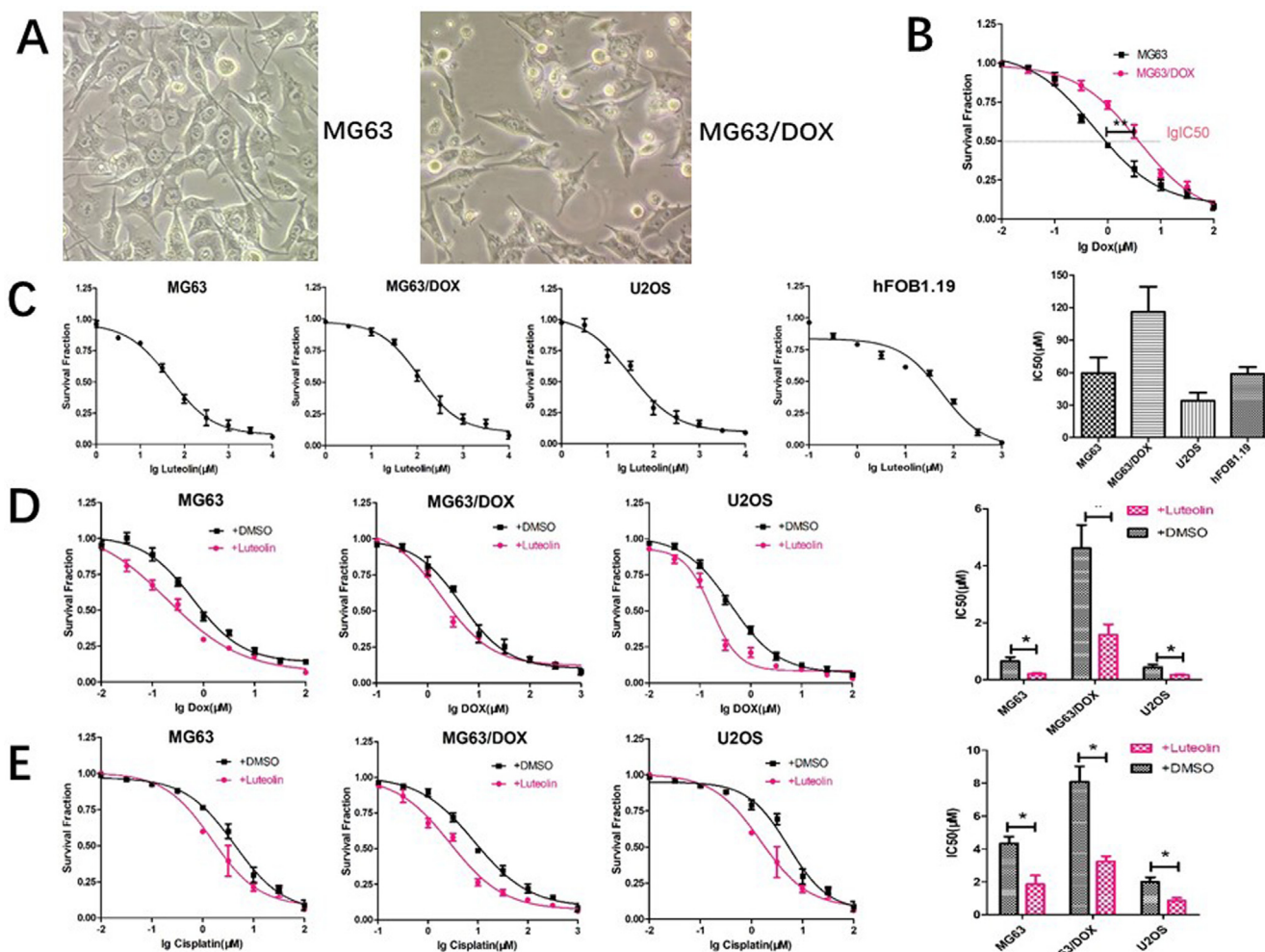
Fig. 1. Effect of luteolin on chemoresistance and miR-384 expression in OS cells. (A) The morphology of MG63 and MG63/DOX cells. (B) Cell viability assay of parental MG63 and resistant MG63/DOX cells followed by doxorubicin treatment at the indicated concentrations. (C) The proliferative inhibition effects of luteolin on human osteosarcoma cells and human osteoblast cell line (hFOB1.19). After exposure to various concentrations (1–1000 μM) of luteolin for 48 h, the cell viability of cells was determined using the CCK-8 assay. The viability ratio decreased in a dose-dependent manner (*P < 0.01 compared with the untreated control group). (D) Luteolin enhances the chemosensitivity of OS cells to doxorubicin. (E) Luteolin enhances the chemosensitivity of OS cells to cisplatin.

the protein level of PTN, indicating a potential negative association between miR-384 and PTN (Fig. 2D).

To further examine whether miR-384 directly targets PTN, we constructed the miR-384 inhibitor/mimics and confirmed their effects on miR-384 expression in OS cells (Fig. 2E). Moreover, luciferase reporter assays were performed in MG63 cells co-transfected with miR-384 mimics, miR-384 mimic NC oligonucleotides, and reporter plasmids (pmir-PTN-WT or pmir-PTN-Mut). As shown in Fig. 2F, miR-384 mimics dramatically reduced the luciferase activity of pmir-PTN with the wild-type 3′-UTR of PTN. Nevertheless, miR-384 mimics failed to influence luciferase activity in the mutant construct. These results indicated that miR-384 directly modulates the expression of PTN by binding to its 3′-UTR.

3.3. miR-384 attenuates OS cell chemoresistance through targeting PTN in vitro

To explore the relationship between miR-384 and PTN as well as their roles in regulating chemoresistance, we downregulated the PTN expression with PTN shRNA transfection and the chemosensitivity assay revealed that silencing PTN could sensitize

OS cells to doxorubicin and cisplatin (Fig. 3A). However, the miR-384 inhibitor could not significantly rescue the low PTN expression caused by PTN shRNA, and the cell viability assay demonstrated that miR-384 silencing failed to reverse the decreased chemoresistance caused by PTN inhibition (Fig. 3A and 3B). Similarly, we ectopically overexpressed PTN by transfecting cDNA that contained the PTN open reading frame without the 3′-UTR. We found that upregulation of PTN significantly enhanced doxorubicin and cisplatin resistance in both MG63 and U2OS cells, and miR-384 mimics could not reverse the PTN upregulation (Fig. 3C). Although an inconspicuous downregulation in the chemoresistance of OS cells treated with miR-384 mimics was observed after PTN expression was upregulated, the results were not statistically significant (Fig. 3C and 3D).

We next detected whether miR-384 modulated OS sensitivity through directly targeting PTN. We found that PTN silencing could significantly reverse the effect of PTN upregulation and chemoresistance enhancement caused by miR-384 inhibition (Fig. 4A and 4B). Similarly, PTN overexpression by transfecting the PTN-carrying vector rescued the downregulation of PTN expression induced by miR-384 mimics (Fig. 4C). Consistently, miR-384 mimics dramatically suppressed PTN expression and sensitized MG63
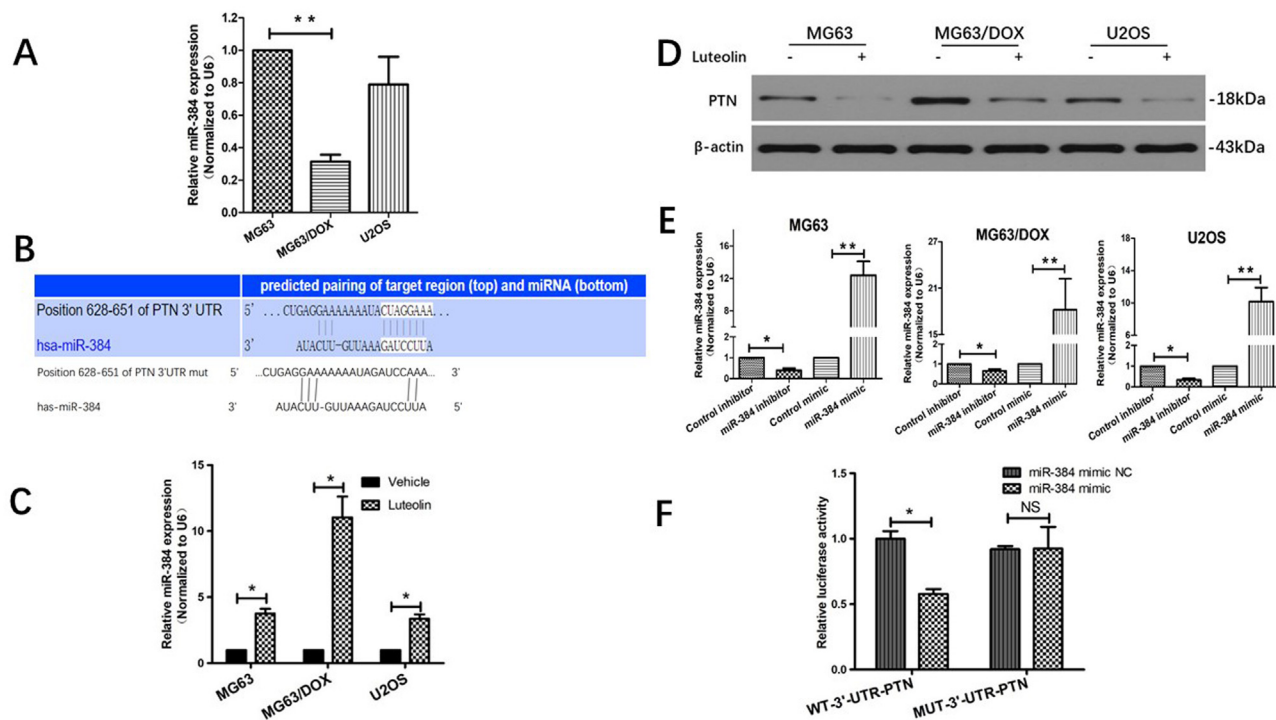
Fig. 2. PTN is a direct target of miR-384 in osteosarcoma. (A) The endogenous expression levels of miR-384 in OS cell lines were analyzed by quantitative RT-PCR (U6 primer was used as the reference, and miR-384 expression in MG63 cells was used as the baseline). (B) miR-384 was predicted to bind to the 3′-UTR of PTN mRNA according to TargetScan analysis. (C) Effect of luteolin on the expression of miR-384 in MG63,MG63/DOX and U2OS cells. (D) Effect of luteolin on PTN expression in OS cells. (E) Expression of miR-384 was examined by qRT-PCR after transfected with miR-384 mimic, miR-384 inhibitor or negative control. (F) A luciferase assay was used to determine whether miR-384 directly targeted PTN. NC, negative control; WT, wide type; MUT, mutant.

and U2OS cells to chemotherapeutic agents, whereas PTN upregulation restored the drug resistance of miR-384-overexpressing OS cells (Fig. 4D).

Since apoptosis inhibition is one of the mechanisms leading to chemoresistance, we detected the effect of miR-384 on drug-induced apoptosis using flow cytometry. As shown in Fig. 5, after cells were incubated with 0.2 μM doxorubicin or 2 μM cisplatin for 24 h, miR-384 mimic significantly increased the apoptosis rates of MG63, MG63/DOX and U2OS cells.

3.4. Luteolin attenuates OS chemoresistance through inhibiting the PTN/β-catenin/MDR1 signaling axis by upregulating miR-384

To further clarify the mechanisms of luteolin, we examined the effect of miR-384 and found that miR-384 inhibitor could significantly increase the protein levels of PTN, anaplastic lymphoma kinase (ALK), p-glycogen synthase kinase (GSK)3β, β-catenin and multidrug resistance protein 1/P-glycoprotein (MDR1/P-gp) compared to the negative control in MG63 cells (Fig. 6A). Meanwhile, the expression of PTN and the downstream ALK/GSK3β/β-catenin/MDR1 signaling pathway could be downregulated with the addition of miR-384 mimics in MG63 cells. Since ALK/GSK3β/β-catenin/MDR1 signaling axis has been demonstrated to be the downstream signaling pathway of PTN in modulating drug resistance of OS cells in our previous study [18], we then only examined the expression of key molecular β-catenin in the following assays. We observed that miR-384 mimics could significantly downregulate the β-catenin expression in both MG63/DOX and U2OS cells (Fig. 6B and 6C). Nevertheless, miR-384 inhibitor could only upregulate β-catenin expression in U2OS cells, largely because β-catenin expression is already extremely high in the chemo-resistant MG63/DOX cells demonstrated in our former study (Fig. 6B) [18].

In chemosensitivity assay, overexpression of miR-384 by miR-384 mimics sensitized MG63, MG63/DOX and U2OS cells to doxorubicin and cisplatin (Fig. 6A-C). Similarly, inhibition of miR-384 by the inhibitor could only dramatically increased IC50 values for these chemotherapeutic agents in MG63 and U2OS cells (Fig. 6A and 6C). The miR-384 inhibitor failed to upregulate the chemoresistance of MG63/DOX cells, largely due to their inherent high chemoresistance (Fig. 6B).

To further explore whether luteolin functions through miR-384 and its target PTN gene, we firstly treated OS cells with luteolin and observed a decrease of PTN expression and chemoresistance to doxorubicin and cisplatin. We found that miR-384 inhibitor could reverse the downregulation of PTN caused by luteolin and result in a restoration of decreased IC50 values induced by luteolin. Similarly, PTN overexpression could restore the luteolin-induced suppression of PTN expression and rescue the decreased chemoresistance caused by luteolin (Fig. 6D-F).

3.5. Luteolin increases the chemosensitivity of chemoresistant OS cells through exosome-transmitted miR-384

Since exosome transduction is a well-established molecular event driving the chemoresistance of many cancer types, we performed a series of assays to determine whether luteolin modulates the chemoresistance via exosomes. To explore whether miR-384 conferred doxorubicin sensitivity through incorporating into exosomes, we detected the existence pattern of extracellular and intracellular miR-384. MiR-384 level in culture medium was unchanged when treated with RNase A alone but significantly decreased upon treatment with RNase A and Triton × 100 simultaneously, indicating that miR-384 was protected by the membrane instead of being released directly (Fig. 7A). Extracellular exosomes
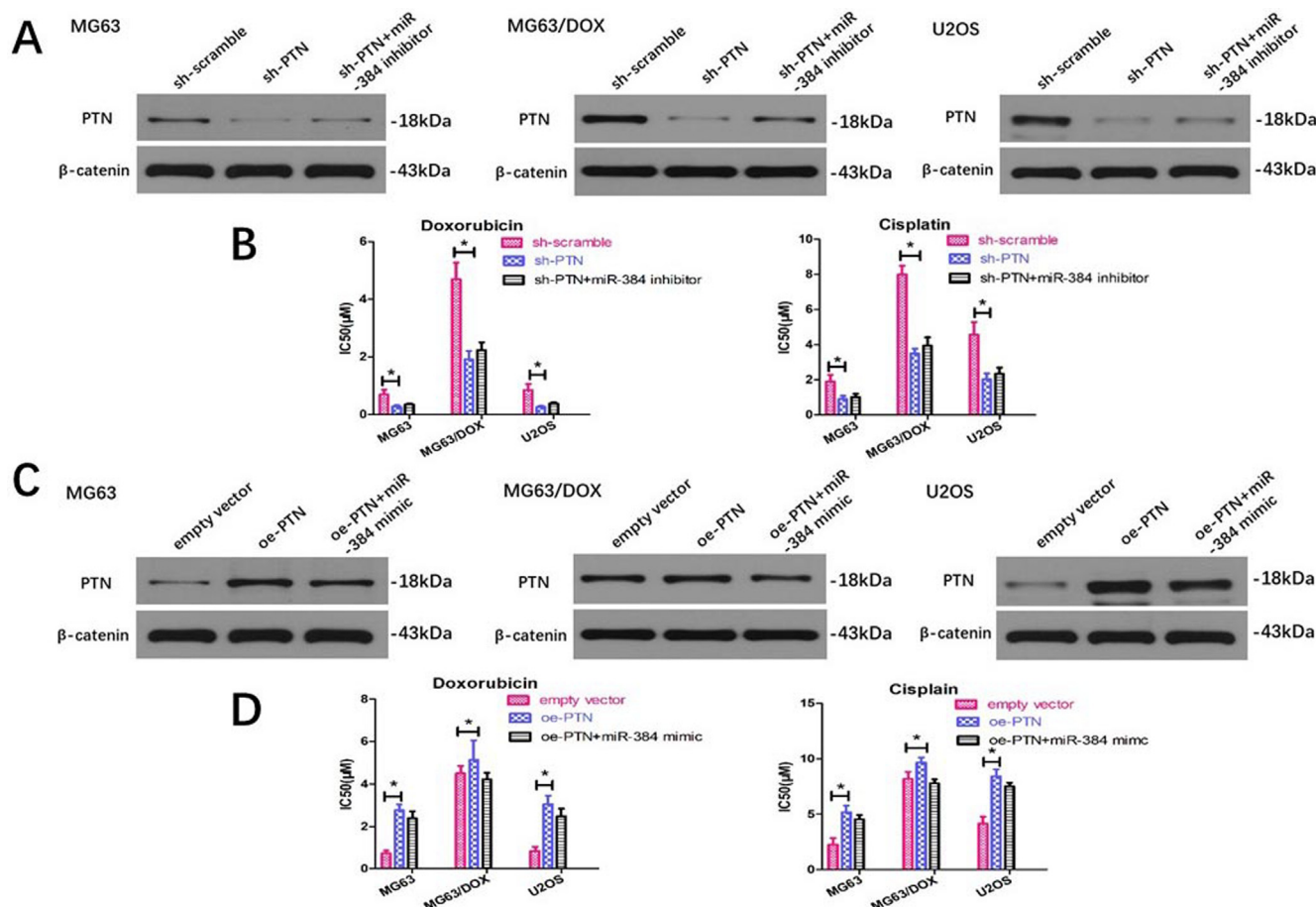
Fig. 3. PTN regulates the chemoresistance of OS cells while these effects could not be significantly reversed by miR-384 modulation. (A) PTN knockdown reduced the expression of PTN and downregulated the chemoresistance to chemotherapeutic agents, while miR-384 inhibitor could not significantly reverse this effect. (B) PTN overexpression upregulated the expression of PTN and downregulated the chemoresistance to chemotherapeutic agents, while miR-384 mimic could not significantly reverse this effect. miR, microRNA; sh, short hairpin RNA; oe, overexpressing.

were isolated from the supernatant of MG63 cells treated with luteolin or control DMSO. They were identified by their typical round or "saucer shape" through transmission electron microscopy and their characteristic sizes ranging from 40 nm to 150 nm in diameter through the nanoparticle tracking analysis (Fig. 7B). Western blot analysis demonstrated that the exosome protein markers, CD63 and CD81, were enriched in exosomes but not in cell extracts (Fig. 7C).

Next, we validated the effect of luteolin on the miR-384 expression in exosomes. qRT-PCR revealed that the level of miR-384 in exosomes derived from luteolin-treated MG63 cells was significantly higher than exosomes derived from MG63 cells treated with the control DMSO (Fig. 7D). Thus, we reasoned that miR-384 may modulate the chemoresistance via exosomal transfer. To visualize exosomal transfer, the MG63-derived exosomes labeled with the membrane phospholipid dye PKH67 were incubated with MG63/DOX cells labeled with DAPI. Fluorescence microscopy confirmed that most of the MG63/DOX cells were positive for PKH67 fluorescence after incubation for 24 h, suggesting that these exosomes were effectively internalized by recipient MG63/DOX cells (Fig. 7E). Furthermore, we observed a significant elevation of miR-384 levels and decreased PTN expression in MG63/DOX cells after treatment with exosomes derived from MG63 cells incubated with luteolin (Fig. 7F). These results demonstrated MG63 cells treated with luteolin could efficiently secrete exosomes containing miR-384 that can be directly transferred into MG63/DOX cells. We next explored whether these exosomes could alleviate

chemoresistance in MG63/DOX cells. In a cell viability assay, MG63/DOX cells incubated with exosomes derived from luteolin-treated MG63 cells elevated the doxorubicin sensitivity of MG63/DOX cells (Fig. 7G).

Lastly, we explored whether miR-384 is transferred via exosomes using a co-culture system with a 0.4 μm pore membrane, which could allow the transmission of exosomes instead of larger particles and avoid direct contact between cells. MG63 cells transfected with miR-384 mimics or scramble control were placed in the upper chamber and MG63/DOX cells were seeded in the lower chamber of the co-culture system (Fig. 7H). We observed miR-384 was dramatically upregulated and PTN expression was markedly downregulated in MG63/DOX cells after co-incubation with miR-384 mimic- transfected MG63 cells. However, when we treated the MG63 cells with the nSMase inhibitor GW4869, the effects of miR-384 mimics in MG63 cells on the expression of miR-384 and PTN in MG63/DOX cells were inhibited (Fig. 7I). In cell viability assays, overexpression of miR-384 in MG63 cells could decrease the chemoresistance to doxorubicin in MG63/DOX cells through exosomes in a co-culture system and this effect could be reversed by inhibiting exosome release from parental MG63 cells by GW4869 (Fig. 7J).

3.6. Effect of luteolin on OS chemoresistance in vivo

To further explore the effects of luteolin on the chemoresistance of osteosarcoma *in vivo*, doxorubicin-resistant MG63/DOX cells
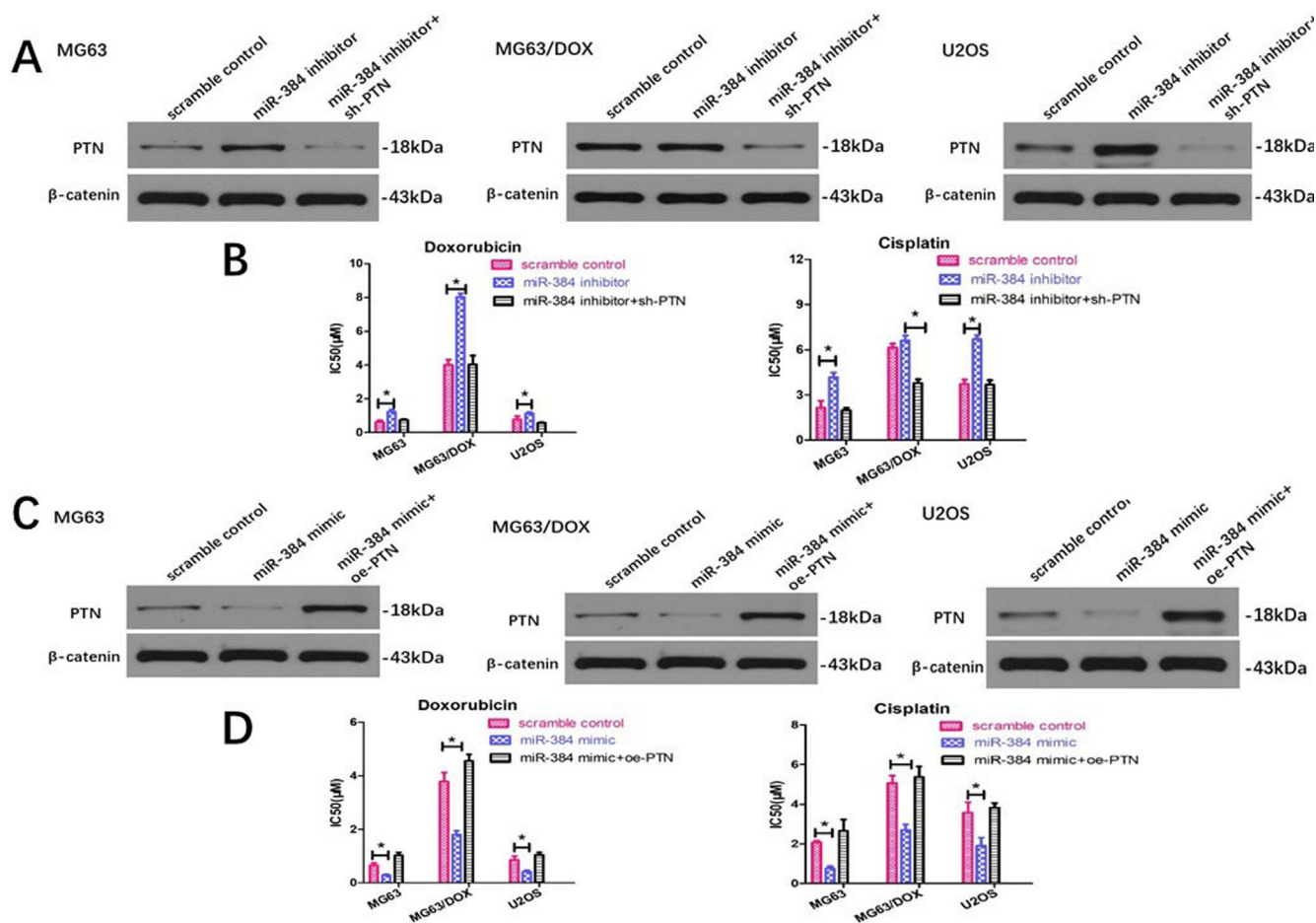
Fig. 4. miR-384 regulates PTN expression and chemoresistance to chemotherapeutic agents, and these effects could be significantly reversed by PTN modulation. (A) miR-384 inhibitor could increase the expression of PTN and upregulate the chemoresistance to doxorubicin and cisplatin, while PTN downregulation could significantly reverse this effect. (B) miR-384 mimics could decrease the expression of PTN and downregulate the chemoresistance to chemotherapeutic agents, while PTN overexpression could significantly reverse this effect.

were employed to build *in vivo* models in 6-week-old BALB/c-nu mice. When the volume of xenograft tumors reached approximately 100 mm^3(day 0), four groups of mice were treated respectively as follows: (1) Control group: injecting normal saline intraperitoneally every 7 days; (2) Doxorubicin group: injecting 2 mg/kg doxorubicin intravenously through tail vein once per week; (3) Luteolin group: injecting 30 mg/kg luteolin intraperitoneally every other day; (4) Combination group: injecting 2 mg/kg doxorubicin intravenously every 7 days + 30 mg/kg luteolin intraperitoneally every other day (Fig. 8A). Since mice began to successively die after day 16 in the four groups, we chose day 16 as a time point for comparison. Compared with the control group, the tumor sizes of both doxorubicin group and luteolin group increased more slowly, while the differences were not significant at day 16 (P = 0.3072 and 0.093, respectively, Fig. 8B). However, xenograft tumors in the combination group had significant poorer growth compared with both the control group and the doxorubicin group at day 16 (P = 0.002 and 0.041, respectively). Moreover, combination therapy of doxorubicin and luteolin resulted in survival of five of six mice while the survival rate was one of six in the control group, two of six in the doxorubicin group and three of six in the luteolin group at study termination (day 28), suggesting luteolin could enhance the anti-tumor effect in combination with doxorubicin (Fig. 8C). The expressions of miR-384, PTN, β-catenin and P-glycoprotein under different treatments were also evaluated using qRT-PCR and immunohistochemistry analysis. There were no sig-

nificant changes in levels of miR-384, PTN, β-catenin and P-glycoprotein in doxorubicin group compared to control. However, upregulation of miR-384 and downregulation of PTN, β-catenin, and P-glycoprotein were observed in the luteolin group and combination group (Fig. 8D and 8E). These results showed luteolin had doxorubicin resistance reversal effect and could potentiate the antitumor effect of doxorubicin *in vivo*.The underlying mechanisms of the effect were summarized in (Fig. 9).

4. Discussion

Although chemotherapy has dramatically improved the therapeutic efficacy of osteosarcoma, the survival rates remain stagnant, largely due to the development of multi-drug resistance [27]. Previous studies have highlighted the molecular mechanisms of multidrug resistance in OS, such as ATP-binding cassette (ABC) transporters, apoptosis inhibition, detoxification in the cell, repair of DNA damage, noncoding RNAs and tumor stem cells, et al. [28] Among these mechanisms, overexpression of P-gp which belongs to the ABC transporter superfamily is considered to be the leading classical cause of multidrug resistance in OS cells [29]. In our previous study, we demonstrated that P-gp could be upregulated by PTN overexpression through the ALK/GSK3β/β-catenin/MDR1 signaling pathway, leading to the augmented drug resistance of osteosarcoma. In the current study, we aimed to explore
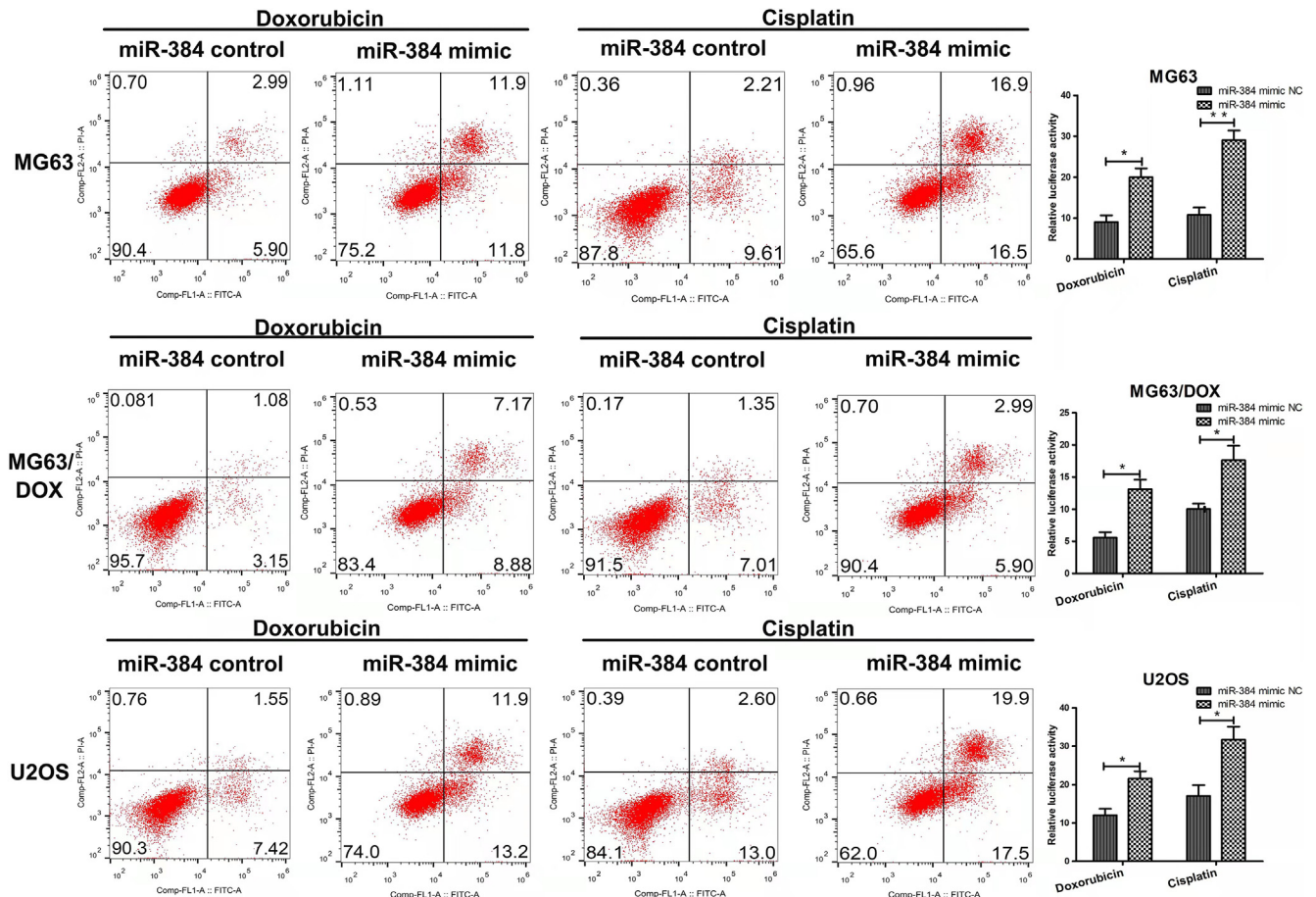
Fig. 5. Flow cytometry for cell apoptosis analysis. MG63, MG63/DOX, and U2OS cells transfected with miR-384 mimics or scramble control were treated with doxorubicin or cisplatin. Cell apoptosis rates were measured using Annexin V-FITC/PI double staining. PI, propidium iodide. Left, representative analysis by FACS. Right, data are presented as the mean ± SD from three independent experiments.
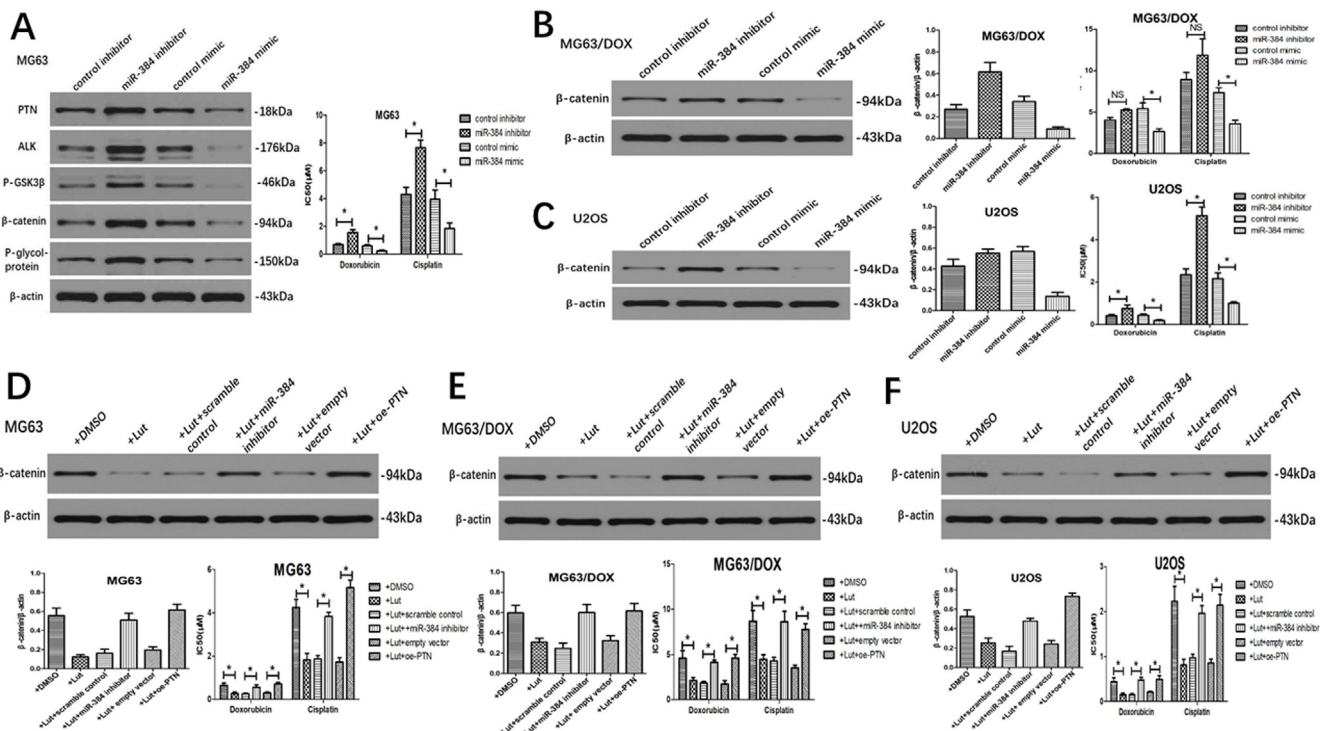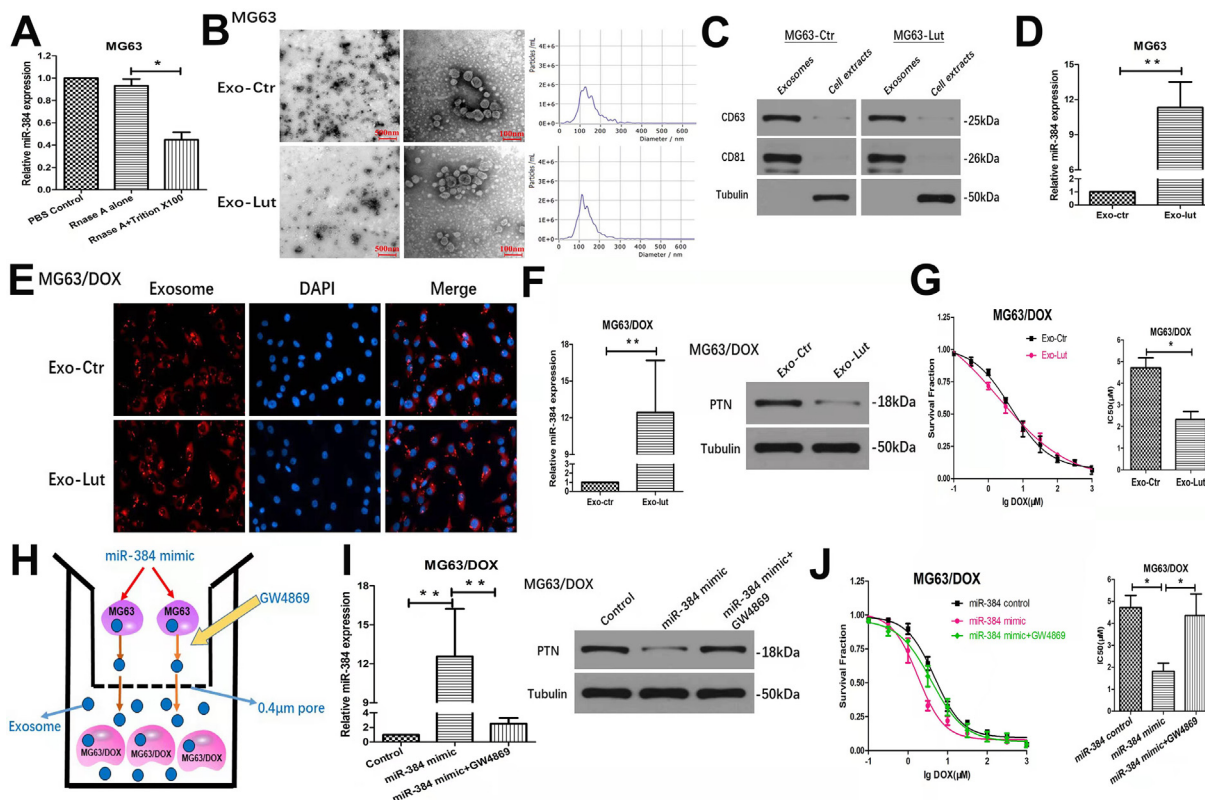
Fig. 7. Luteolin modulates chemosensitivity of OS cells through exosome-transmitted miR-384. (A) qRT-PCR analysis of extracellular miR-384 of MG63 cells treated with RNase A (10 µg/ml) or the combination of RNase A and 0.3% Triton X-100. *P < 0.05 compared with RNase A group. (B) Left: Representative transmission electron microscopy images of cup-shaped exosomes released by MG63 cells. Scale bar = 500 nm and 100 nm, respectively. Right: Nanoparticle tracking analysis on the size distribution and relative concentration of exosomes derived from MG63 cells using the Nano-sight software. (C) Western blotting of exosomal protein markers (CD63 and CD81) from purified exosomes and cell extracts. (D) qRT-PCR detection of miR-384 expression in exosomes derived from MG63 cells treated with DMSO or luteolin. (E) Representative fluorescence microscopy images showing cellular uptake of exosomes (PKH67-labeled, red) into recipient MG63/DOX cells (DAPI-labelled, blue). (F) Effect of specified exosomes on the expression of miR-384 and PTN in recipient MG63/DOX cells. Exosomes were derived from MG63 cells treated with or without luteolin and then incubated with MG63/DOX cells. (G) Effect of specified exosomes on the chemoresistance of recipient MG63/DOX cells by cell viability analysis. MG63/DOX cells co-cultured with exosomes from MG63 cells were treated with a series of concentrations of doxorubicin for 48 h and cell growth was assessed by CCK-8 assay. (H) Schematic diagram of the co-culture system. MG63 cells transfected with miR-NC or miR-384 mimic plasmids were seeded in the upper chamber and co-incubated with MG63/DOX cells placed in the lower chamber in a co-culture system with a 0.4 µM pore membrane. Then the MG63 cells were treated with the nSMase inhibitor GW4869 or control DMSO. (I) MG63 cells transfected with miR-384 mimics could increase the miR-384 level and downregulate the PTN level in MG63/DOX cells in a co-culture system and this effect could be significantly attenuated by 10 µM GW4869. (J) CCK-8 assay was used to assess the chemoresistance of MG63/DOX cells after co-culturing with miR-384 mimic-transfected MG63 cells with or without GW4869 treatment. DAPI, 4′,6-diamidino-2-phenylindole; Exo, exosome; Lut, luteolin; ctr: control. (For interpretation of the references to colour in this figure legend, the reader is referred to the web version of this article.)

the effect of luteolin on OS and then explored whether luteolin could function through the PTN/β-catenin/MDR1 axis.

Compounds extracted from natural products, with relatively smaller side effects, provide one of the most promising and diverse scaffolds for the development of new antitumor drugs [30]. It is noted that flavonoids are the most well-known modulators of several ABC transporters including P-gp [30]. As a kind of flavonoid, luteolin has been confirmed to exhibit chemosensitising or chemo-

Fig. 6. Luteolin attenuates the chemoresistance by downregulating P-gp through inhibiting the PTN/ALK/GSK3β/β-catenin signaling pathway. (A) miR-384 mimics reduced the expression of PTN, ALK, p-GSK3β, β-catenin, and P-gp in MG63 cells, while miR-384 inhibitor enhanced their expression. miR-384 mimic impaired the chemoresistance to doxorubicin and cisplatin, while miR-384 inhibitor enhanced the chemoresistance in MG63 cells. (B) miR-384 mimics reduced the expression of β-catenin and impaired the chemoresistance to doxorubicin in MG63/DOX cells, while the effects of miR-384 inhibitor on β-catenin expression and chemoresistance were not significant. (C) miR-384 mimics reduced the expression of β-catenin and chemoresistance in U2OS cells, and miR-384 inhibitor enhanced the β-catenin expression and chemoresistance. (D-F) Effect of miR-384 inhibitor and PTN overexpression on β-catenin expression and chemoresistance after luteolin treatment.

preventive properties against various cancers [8]. Studies have suggested that luteolin exerts its action of modulating chemoresistance through several mechanisms. For example, luteolin could enhance the chemosensitivity of Taxol by attenuating the cell stemness features through the Nrf2-mediated pathway in breast cancer [31]. Wang et al. reported that luteolin sensitizes the effect of cisplatin in cisplatin-resistant ovarian cancer via induction of apoptosis [8]. In another investigation, luteolin was reported to promote doxorubicin-induced apoptosis via Bax/Bcl-2/Caspase-3 pathway in triple-negative breast cancer [32]. As a RSK inhibitor, luteolin could also increase the efficacy of chemotherapy through eradicating the population of cancer stem cells [33]. In our experiment, we found the effect of doxorubicin and cisplatin becomes stronger when OS cells are treated with both luteolin and chemotherapeutic drugs than single agent treatment, which is consistent with the results in other types of cancer. Moreover, our study showed luteolin alone failed to exhibit selective cytotoxicity between OS cells and normal osteoblast hFOB1.19 cells due to their approximate IC50 values in luteolin treatment. Since treating tumors effectively with low toxicity is urgently required, we used 1/2 IC50 concentrations of luteolin which repre-
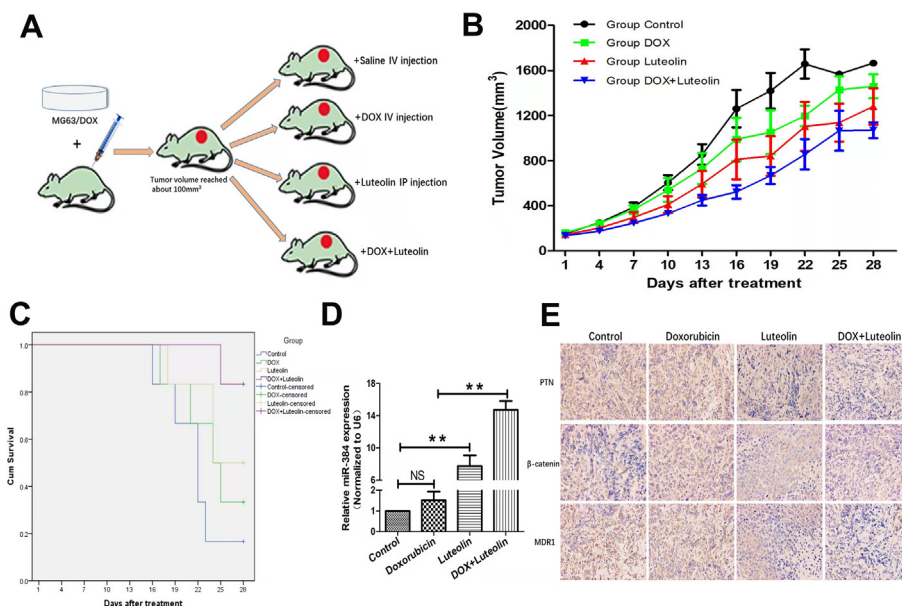
Fig. 8. *In vivo* effect of luteolin and doxorubicin therapy on osteosarcoma. (A) A schematic outline of the experimental design. When the tumor volume reached 100 mm³, mice were treated with normal saline (control), doxorubicin only, luteolin only, and combination of doxorubicin and luteolin, respectively. (B) Growth curves for tumor volume in mice. (C) Kaplan-Meier plot survival time in each group with different treatment. P values were compared using a two-sided log-rank test. (D) RT-qPCR analysis of miR-384 expression in xenograft tumors. (E) Representative IHC images of PTN, β-catenin, and P-glycoprotein staining in xenograft tumor sections at 400× magnification. Positive staining is indicated by the brown color. DOX, doxorubicin.
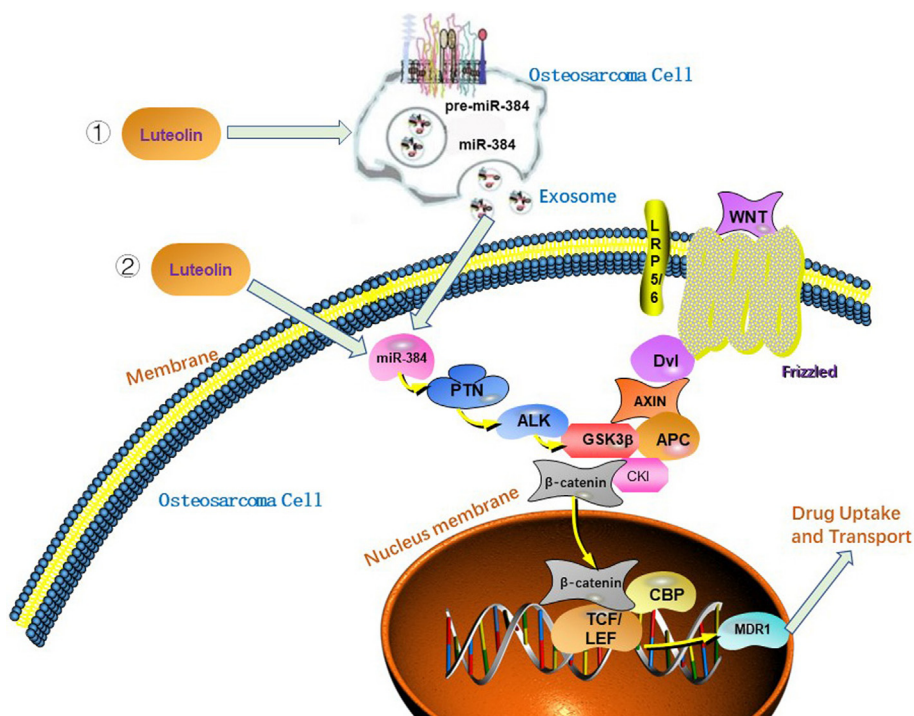

Fig. 9. Schematic diagram showing that luteolin modulates the chemoresistance of osteosarcoma through inhibiting the PTN-guided ALK//β-catenin/MDR1 signaling pathway by upregulating miR-384.

sented lower cytotoxicity to normal cells as study concentrations. These concentrations of luteolin successfully showed synergistic effects with chemotherapeutic drugs in our research and further dose-dependent studies are needed to explore the best concentra-

tions of luteolin that could both minimize the cytotoxicity and maximize the effect of attenuating chemoresistance in OS cells.

As a heparin-binding growth factor, PTN has been demonstrated to be overexpressed and served as an oncogene in several cancers

[34–35]. Our previous study has verified that high PTN expression correlated with poor overall and disease-free survival of OS patients, and PTN could promote the chemoresistance of osteosarcoma by upregulating P-gp [18]. Another study by our team also indicated PTN inhibition lowered doxorubicin resistance in OS cells [19]. These results both indicated the vital role of PTN in modulating chemoresistance in osteosarcoma. Thus, we wondered whether luteolin could function through PTN in osteosarcoma. As a kind of small noncoding RNAs, miRNAs are thought to modulate specific target genes that are implicated in various cellular processes. In our research, PTN was identified as a direct target of miR-384 by the bioinformatic analysis, dual luciferase reporter assay, gain-of-function and loss of-function assays, which coincided with the study conducted by Yao et al. [20] Recent studies indicated that miR-384 acts as a tumor suppressor in several types of human malignant tumors. It could inhibit cell viability, invasion, migration and promote apoptosis in many tumors such as gastric cancer, colorectal cancer, non-small cell lung cancer, nasopharyngeal carcinoma, glioma, papillary thyroid cancer, prostate cancer, pancreatic cancer, et al. [36–43] In osteosarcoma, there is also some evidence that miR-384 could promote apoptosis and exert suppressive effect on cell proliferation, invasion, and migration [24–26]. In our work, we found that miR-384 could enhance the apoptosis induced by doxorubicin or cisplatin in OS cells. We verified that luteolin could upregulate the expression of miR-384 and miR-384 is downregulated in chemoresistant OS cell lines compared with the parental sensitive cell lines. In addition, we confirmed luteolin could modulate miR-384 and identified a regulatory relationship between miR-384 and PTN. To the best of our knowledge, our study is the first to exhibit the underlying mechanisms luteolin influences chemoresistance in osteosarcoma.

After clarifying the regulatory role of miR-384 in OS cells, we wondered whether miR-384 could disseminate its antiresistant function through the intercellular interaction. Exosome is a means of intracellular communication via the transport of biological cargoes, comprising mRNAs, miRNAs, and proteins [44]. miRNAs could be encapsulated in exosomes to avoid degradation and then shuttled to recipient cells to modify their phenotypes through changing the expression of target genes [45]. Mounting evidence suggested that tumor-derived exosomes could reverse or spread chemoresistance among heterogeneous populations of tumor cells. Therefore, these extracellular exosomes play a pivotal role in tumor chemoresistance and may ultimately influence therapeutic efficiency [46]. In our study, we firstly confirmed that the expression of miR-384 in exosomes was upregulated after luteolin treatment. Then we used the pore membrane of the transwell chamber to inhibit direct contact between two groups of cells, which only allowed the lower chamber cells to coculture with exosomes with the help of gravity. We observed that the sensitivity conferred by exosomes from sensitive OS cells was sustainable, possibly owing to the triggering of a PTN/MDR1-based signaling pathway inhibition in recipient resistant cells. A subsequent functional assay with a nSMase inhibitor (GW4869) further confirmed the role of exosomes. Based on these findings, we confirmed that luteolin could attenuate the chemoresistance of resistant cells by exosomes secreted from sensitive cells, and miR-384 could function through incorporating it into exosomes in parental sensitive cells and then transfer into recipient resistant cells.

Taken together, our research study confirmed that luteolin could attenuate the chemoresistance of osteosarcoma through inhibiting the PTN/β-catenin/MDR1 signaling axis by upregulating miR-384. Our research also demonstrated that doxorubicin resistance could be inhibited by the transfer of exosomal miR-384 into recipient OS cells. Our study shed light on the mechanisms that luteolin exerts its effects on drug resistance, which may be valuable for translational application of luteolin and design of novel drugs in the future.

Declaration of Competing Interest

The authors declare that they have no known competing financial interests or personal relationships that could have appeared to influence the work reported in this paper.

Acknowledgments

Author contributions

Tao Qin and Dapeng Wu designed the research processes. Tao Qin, Wenjing Zhu and Xiaoli Kan performed the experiments and analyzed the data. Xiaoli Kan and Ling Li wrote the manuscript. Dapeng Wu revised the manuscript and supervised the whole study.

References

[1] X. Zhao, Q. Wu, X. Gong, et al., Osteosarcoma: a review of current and future therapeutic approaches, Biomed. Eng. Online 20 (1) (2021).
[2] Y. Lin, R. Shi, X. Wang, H.M. Shen, Luteolin, a flavonoid with potential for cancer prevention and therapy, Curr. Cancer Drug Targets 8 (2008) 634–646.
[3] L. Franza, V. Carusi, E. Nucera, F. Pandolfi, Luteolin, inflammation and cancer: special emphasis on gut microbiota, BioFactors 47 (2) (2021) 181–189.
[4] A. Hosseini, A. Sahebkar, Reversal of doxorubicin-induced cardiotoxicity by using phytotherapy: a review, J. Pharmacopuncture 20 (2017) 243–256.
[5] M. Imran, A. Rauf, T. Abu-Izneid, et al., Luteolin, a flavonoid, as an anticancer agent: a review, Biomed. Pharmacother. 112 (2019) 108612.
[6] E. Seydi, A. Salimi, H.R. Rasekh, et al., Selective cytotoxicity of luteolin and kaempferol on cancerous hepatocytes obtained from rat model of hepatocellular carcinoma: involvement of ROS-mediated mitochondrial targeting, Nutr. Cancer 70 (4) (2018) 594–604.
[7] N. Kittiratphatthana, V. Kukongviriyapan, A. Prawan, et al., Luteolin induces cholangiocarcinoma cell apoptosis through the mitochondrial-dependent pathway mediated by reactive oxygen species, J. Pharm. Pharmacol. 68 (9) (2016) 1184–1192.
[8] H. Wang, Y. Luo, T. Qiao, et al., Luteolin sensitizes the antitumor effect of cisplatin in drug-resistant ovarian cancer via induction of apoptosis and inhibition of cell migration and invasion, J. Ovarian Res. 11 (1) (2018) 93.
[9] K.C. Tjioe, D. Tostes Oliveira, et al., Luteolin impacts on the DNA damage pathway in oral squamous cell carcinoma, Nutr. Cancer 68 (5) (2016) 838–847.
[10] S. Chian, Y.Y. Li, X.J. Wang, et al., Luteolin sensitizes two oxaliplatin-resistant colorectal cancer cell lines to chemotherapeutic drugs via inhibition of the Nrf2 pathway, Asian Pac. J. Cancer Prev. 15 (6) (2014) 2911–2916.
[11] Q. Qu, J. Qu, Y. Guo, et al., Luteolin potentiates the sensitivity of colorectal cancer cell lines to oxaliplatin through the PPARγ/OCTN2 pathway, Anticancer Drugs 25 (9) (2014) 1016–1027.
[12] Y.J. Lee, T. Lim, M.S. Han, et al., Anticancer effect of luteolin is mediated by downregulation of TAM receptor tyrosine kinases, but not interleukin-8, in non-small cell lung cancer cells, Oncol. Rep. 37 (2) (2017) 1219–1226.
[13] Z.C. Liu, K. Cao, Z.H. Xiao, et al., VRK1 promotes cisplatin resistance by up-regulating c-MYC via c-Jun activation and serves as a therapeutic target in esophageal squamous cell carcinoma, Oncotarget 8 (39) (2017) 65642–65658.
[14] J. Zhao, L. Li, Z. Wang, et al., Luteolin attenuates cancer cell stemness in PTX-resistant oesophageal cancer cells through mediating SOX2 protein stability, Pharmacol. Res. 174 (2021) 105939.
[15] Y. Wang, D. Kong, X. Wang, et al., Molecular mechanisms of luteolin induced growth inhibition and apoptosis of human osteosarcoma cells, Iran J. Pharm. Res. 14 (2) (2015) 531–538.
[16] B. Zhang, X. Yu, H. Xia, The flavonoid luteolin enhances doxorubicin-induced autophagy in human osteosarcoma U2OS cells, Int. J. Clin. Exp. Med. 8 (9) (2015) 15190–15197.
[17] J. Zhou, Y. Yang, Y. Zhang, et al., A meta-analysis on the role of pleiotrophin (PTN) as a prognostic factor in cancer, PLoS ONE 13 (11) (2018) e0207473.
[18] D. Wu, L. Liu, X. Yan, et al., Pleiotrophin promotes chemoresistance to doxorubicin in osteosarcoma by upregulating P-glycoprotein, Oncotarget 8 (38) (2017) 63857–63870.
[19] X. Sun, C. Tian, H. Zhang, et al., Long noncoding RNA OIP5-AS1 mediates resistance to doxorubicin by regulating miR-137-3p/PTN axis in osteosarcoma, Biomed. Pharmacother. 128 (2020) 110201.

[20] Y. Yao, C. Rao, G. Zheng, S. Wang, Luteolin suppresses colorectal cancer cell metastasis via regulation of the miR–384/pleiotrophin axis, Oncol. Rep. 42 (1) (2019) 131–141.

[21] K. Han, W. Meng, J.J. Zhang, et al., Luteolin inhibited proliferation and induced apoptosis of prostate cancer cells through miR-301, Onco Targets Ther. 9 (2016) 3085–3094.

[22] Y. Zhou, B.Z. Ding, Y.P. Lin, H.B. Wang, MiR-34a, as a suppressor, enhance the susceptibility of gastric cancer cell to luteolin by directly targeting HK1, Gene 644 (2018) 56–65.

[23] G. Gao, R. Ge, Y. Li, S. Liu, Luteolin exhibits anti-breast cancer property through up-regulating miR-203, Artif. Cells Nanomed. Biotechnol. 47 (1) (2019) 3265–3271.

[24] Y. Wang, H. Huang, Y. Li, Knocking down miR-384 promotes growth and metastasis of osteosarcoma MG63 cells by targeting SLBP, Artif. Cells Nanomed. Biotechnol. 47 (1) (2019) 1458–1465.

[25] J.F. Zhang, G.Y. Zhang, X.M. Hu, et al., MicroRNA-384 downregulates SETD8 expression to suppress cell growth and metastasis in osteosarcoma cells, Eur. Rev. Med. Pharmacol. Sci. 22 (6) (2018) 1602–1608.

[26] Y. Tan, L. Chen, S. Li, et al. MiR-384 Inhibits malignant biological behavior such as proliferation and invasion of osteosarcoma by regulating IGFBP3. *Technol. Cancer Res. Treat.* 2020;19: 1533033820909125.

[27] I. Buondonno, E. Gazzano, S.R. Jean, et al., Mitochondria-targeted doxorubicin: a new therapeutic strategy against doxorubicin-resistant osteosarcoma, Mol. Cancer Ther. 15 (11) (2016) 2640–2652.

[28] S. Li, W. Sun, H. Wang, et al., Research progress on the multidrug resistance mechanisms of osteosarcoma chemotherapy and reversal, Tumour Biol. 36 (3) (2015) 1329–1338.

[29] D. Brambilla, S. Zamboni, C. Federici, et al., P-glycoprotein binds to ezrin at amino acid residues 149–242 in the FERM domain and plays a key role in the multidrug resistance of human osteosarcoma, Int. J. Cancer 130 (12) (2012) 2824–2834.

[30] C.P. Wu, S. Ohnuma, S.V. Ambudkar, Discovering natural product modulators to overcome multidrug resistance in cancer chemotherapy, Curr. Pharm. Biotechnol. 12 (4) (2011) 609–620.

[31] K.J. Tsai, H.Y. Tsai, C.C. Tsai, et al., Luteolin inhibits breast cancer stemness and enhances chemosensitivity through the Nrf2-mediated pathway, Molecules 26 (21) (2021) 6452.

[32] Y. Shi, F. Li, M. Shen, et al., Luteolin prevents cardiac dysfunction and improves the chemotherapeutic efficacy of doxorubicin in breast cancer, Front. Cardiovasc. Med. 8 (2021) 750186.

[33] A.H. Davies, K. Reipas, K. Hu, et al., Inhibition of RSK with the novel small-molecule inhibitor LJI308 overcomes chemoresistance by eliminating cancer stem cells, Oncotarget 6 (24) (2015) 20570–20577.

[34] C. Xu, Y. Wang, Q. Yuan, et al., Serum pleiotrophin as a diagnostic and prognostic marker for small cell lung cancer, J. Cell Mol. Med. 23 (3) (2019) 2077–2082.

[35] H. Sun, L. He, L. Ma, et al., LncRNA CRNDE promotes cell proliferation, invasion and migration by competitively binding miR-384 in papillary thyroid cancer, Oncotarget 8 (66) (2017) 110552–110565.

[36] B.Z. Zhong, Q. Wang, F. Liu, et al., Effects of mir-384 and mir-134-5p acting on yy1 signaling transduction on biological function of gastric cancer cells, Onco Targets Ther. 13 (2020) 9631–9641.

[37] B. Li, H. Sun, J. Zhang, LncRNA DSCAM-AS1 promotes colorectal cancer progression by acting as a molecular sponge of miR-384 to modulate AKT3 expression, Aging (Albany NY). 12 (10) (2020) 9781–9792.

[38] Q. Ma, B. Huai, Y. Liu, Z. Jia, Q. Zhao, Circular RNA circ_0020123 promotes non-small cell lung cancer progression through miR-384/TRIM44 Axis, Cancer Manag. Res. 13 (2021) 75–87.

[39] X. Zeng, H. Liao, F. Wang, MicroRNA-384 inhibits nasopharyngeal carcinoma growth and metastasis via binding to Smad5 and suppressing the Wnt/β-catenin axis, Cytotechnology 73 (2) (2021) 203–215.

[40] R. Ma, B.W. Zhang, Z.B. Zhang, Q.J. Deng, LncRNA MALAT1 knockdown inhibits cell migration and invasion by suppressing autophagy through miR-384/GOLM1 axis in glioma, Eur. Rev. Med. Pharmacol. Sci. 24 (5) (2020) 2601–2615.

[41] Y. Wang, B. Wang, H. Zhou, et al., MicroRNA-384 inhibits the progression of papillary thyroid cancer by targeting PRKACB, Biomed Res. Int. 2020 (2020) 1–11.

[42] Z. Hong, W. Fu, Q. Wang, et al., MicroRNA-384 is lowly expressed in human prostate cancer cells and has anti-tumor functions by acting on HOXB7, Biomed. Pharmacother. 114 (2019) 108822.

[43] G. Wang, J. Pan, L. Zhang, et al., Long non-coding RNA CRNDE sponges miR-384 to promote proliferation and metastasis of pancreatic cancer cells through upregulating IRS1, Cell Prolif. 50 (6) (2017) e12389.

[44] A.A. Farooqi, N.N. Desai, M.Z. Qureshi, et al., Exosome biogenesis, bioactivities and functions as new delivery systems of natural compounds, Biotechnol. Adv. 36 (1) (2018) 328–334.

[45] D. Sousa, R.T. Lima, M.H. Vasconcelos, Intercellular transfer of cancer drug resistance traits by extracellular vesicles, Trends Mol. Med. 21 (10) (2015) 595–608.

[46] L. Mashouri, H. Yousefi, A.R. Aref, et al., Exosomes: composition, biogenesis, and mechanisms in cancer metastasis and drug resistance, Mol. Cancer 18 (1) (2019) 75.